

# MODELLING OF THE EARLY AGE SHRINKAGE CRACKS WITH STEEL OR SYNTHETIC MACRO FIBRE REINFORCEMENT IN JOINTLESS FLOORS

JUHÁSZ Károly Péter<sup>1</sup>, NAGY Lóránt<sup>2</sup>, SCHAUL Péter<sup>3</sup>

## Abstract

*The use of fibre reinforcement has become a popular alternative to traditional steel mesh in industrial floors for the control of early age shrinkage. However, there are no generally accepted standards for the design of the jointless floors, only guidelines. One of the most well-known guidelines for industrial floors is the British guideline: TR 34 – Concrete Industrial Ground Floors. In the 4<sup>th</sup> edition the calculation method of early age shrinkage was totally omitted, and the document limits itself to simply stating that cracks could be avoided if the concrete mix design, curing time and dilatation distances are appropriate and well designed. Our research is about the comparison of the early age effect of plain, steel or synthetic macro fibre reinforced concretes with beam test series at different ages: 9-14-24 hours and 7 and 28 days. The results of these tests were implemented into an advanced Finite Element Analysis, with a time-dependent material model which enabled the simulation of the effect of the fibres on the crack propagation during the hardening of the concrete in an industrial floor. The connection to the subbase was modelled with different interface elements to model the slip effect. Results show clearly the difference between plain, steel and synthetic fibre reinforced concrete materials.*

**Keywords:** early age shrinkage; steel fibre; synthetic macro fibre; jointless floors

## 1. Introduction

The shrinkage cracking of concrete due to a high rate of evaporation is a well-known process. Different models are published in the literature. Eurocode [3] and *fib* [4] models are dependent on the relative humidity, drying surface of the structure, concrete strength and cement type. Both codes separate the shrinkage to two parts: autogenous and drying shrinkage. According to Japanese standards [7] the calculation method of shrinkage is different for normal and high strength concrete. For normal concretes the shrinkage depends on the relative humidity, drying surface and water content of the concrete. The calculation method is simpler, but the results are more conservative than in the case of the previous methods. ACI 209 guideline [1] takes into account relative humidity, drying surface, slump of the fresh concrete, ratio of fine aggregate to total aggregate and cement and air content. Results of this guideline fall somewhere between the Japanese and the

---

<sup>1</sup> JUHÁSZ Károly Péter, 1111 Budapest, Műegyetem rkp. 3., Hungary, [juhasz@szt.bme.hu](mailto:juhasz@szt.bme.hu)

<sup>2</sup> NAGY Lóránt, 1135 Budapest, Reitter Ferenc 73. A/5/4, Hungary, [lorant.nagy@jpk.hu](mailto:lorant.nagy@jpk.hu)

<sup>3</sup> SCHAUL Péter, 1135 Budapest, Reitter Ferenc 73. A/5/4, Hungary, [peter.schaul@jpk.hu](mailto:peter.schaul@jpk.hu)

European ones. None of the guidelines above takes into consideration the effect of the fibres.

The fiber reinforcement, both micro and macro from different materials, reduces the crack propagation and crack width due to the shrinkage. Many publications have the same result with different testing methods. Swamy and Stavrides [16] researched steel macro, PP and glass mono micro fibres with restrained ring tests; Shah, Sarigaphuti and Karaguler [14] tested also steel macro and synthetic fibrillated micro fibres with restrained and free shrinkage tests. Józsa and Fenyvesi [8] used micro glass and PP fibres and tested according to the Austrian fibre guideline [12]. Rahmani et.al. [13] used steel macro, glass and polypropylene micro and polyolefin macro fibers by performing ASTM C1579 tests.

Although, the added fibres of different types decrease the crack propagation and crack width of the concrete the effects after the formation of the crack are different. Steel and synthetic macro (depending on the dosage) have significant residual strength after cracking, while the effect of micro (mono and fibrillated) on the residual strength is negligible. To characterize the effect of the fibre on the residual strength the modified fracture energy of the fibre reinforced concrete ( $G_{FRC}$ ) could be used [9]. This fracture energy consists of the fracture energy of the concrete ( $G_f$ ) and the added fracture energy added by the fibres ( $G_{ff}$ ). In this research the alteration of this added fracture energy is investigated by beam test series carried out in different points of time.

## 2. Experimental program and testing

### 2.1 Testing program

Beams moulded at the same time, but tested at different ages by three points bending beam tests were made. From the results of load-deflection curve the fracture energy and added fracture energy could be calculated. The ages of the beams are the followings: 9-14-24 hours and 7 and 28 days. Beams were made according to RILEM TC162 [17], but without notches. Notches would have been difficult to make at early ages, and also the gluing of measuring steel knife edges would have been difficult. From the average of the results the added fracture energy was calculated, which could be used in the finite element material model.

### 2.2 Materials and mix design composition

The concrete mix was designed to model a typical industrial floor concrete. Cement type was CEM III/A-32.5-N, water-cement ratio was 0.49. The mixture design can be seen in Table 1.

Tab.1: Concrete mix

| Concrete name | Cement type    | w/c ratio | Aggregates (kg/m <sup>3</sup> ) |     |      | Admixtures       |
|---------------|----------------|-----------|---------------------------------|-----|------|------------------|
|               |                |           | 0-4                             | 4-8 | 8-16 |                  |
| A             | CEM-III-A-32.5 | 0.492     | 722                             | 380 | 799  | Dynamon SR3 1.63 |

Two different types of fibre reinforcement were used: steel and synthetic macro. The dosages of the fibers were typical: steel fibre of 30 kg/m<sup>3</sup> and synthetic fibre of 2.5 and 5

kg/m<sup>3</sup> were used. The types of the fibres and the research matrix can be seen in Table 2 and 3. Three beams were made in each type.

The aggregate, sand and cement were first mixed while the water was added continuously. Mixing was carried out with Collomatic XM3 forced action mixer. For fibre reinforced concrete the fibers were dispersed by hand and mixed approximately for one minute to achieve a uniform distribution. The concrete was casted into steel formworks and was demoulded after 6 hours. The beams were kept in a temperature of 25 °C, and a relative humidity of 50-60%.

Tab.2: Fibre reinforcing

| Fibre sign/name   | Fibre type                          | Fibre length mm | Dosage kg/m <sup>3</sup> | Number of fibres Number/m <sup>3</sup> |
|-------------------|-------------------------------------|-----------------|--------------------------|--|
| SY25<br>Barchip48 | Synthetic fibre<br>Surface embossed | 48              | 2.5                      | 150 602                                |
| SY50<br>Barchip48 | Synthetic fibre<br>Surface embossed | 48              | 5.0                      | 301 205                                |
| ST30<br>Armfib®   | Steel fibre<br>Hook-end             | 50              | 30                       | 93 780                                 |

Tab.3: Research matrix

| Name of the specimen | Concrete | Fibre |
|----------------------|----------|-------|
| EAS-A-0-time         | A        | -     |
| EAS-A-SY25-time      | A        | SY25  |
| EAS-A-SY50-time      | A        | SY50  |
| EAS-A-ST30-time      | A        | ST30  |

### 2.3 Specimen preparation and testing

Three points unnotched beam tests were used. The load and the middle point deflection were measured. The test was performed by a universal testing machine ZWICK Z150 in the Laboratory of Department of Mechanics, Materials and Structures, Budapest University of Technology and Economics. The speed of the test was 0.2 mm/sec until total failure or 3 mm central deflection.

### 2.4 Test results

The results of the different concretes at different ages can be seen in Fig. 1. From the test the flexural tensile strength ( $f_t$ ), the  $R_{e3}$  number and the fracture energy ( $G_f$ ) could be measured. The  $R_{e3}$  value, a measure of the ductility, is the average load applied as the beam deflects to 3 mm expressed as a ratio of the load to first crack according to the Japanese standard JSCE-SF4 [6]. The compression strength ( $f_c$ ) and the elastic modulus ( $E$ ) were determined according to the literature [18, 5, 15]. The increase of the parameters of the concrete as a function of time could be seen in Fig. 2. The tension strength shows good correlation with the literature. The changes in the  $R_{e3}$  number can be seen in Fig. 3. Here, a significant difference could be seen between the steel and synthetic reinforcement, namely the ductility increases with time in case of steel fibre, while it decreases in case of synthetic fibre. On the other hand it means that only synthetic fibre could work effectively

at early ages, during the beginning part of the hardening. As early-age cracks occur between 2 and 20 hours therefore only synthetic fibre can prevent crack opening in this range.

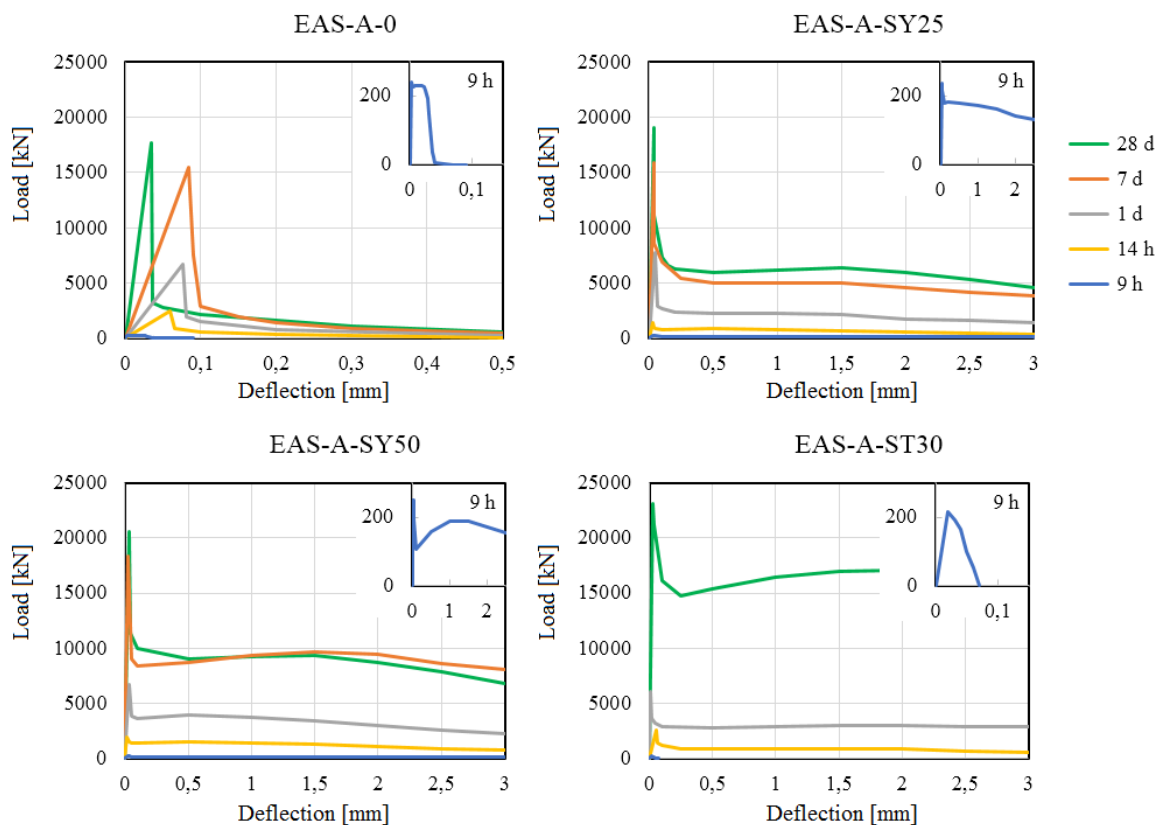


Fig. 1: Average test results of plain and fibre reinforced concretes at different ages

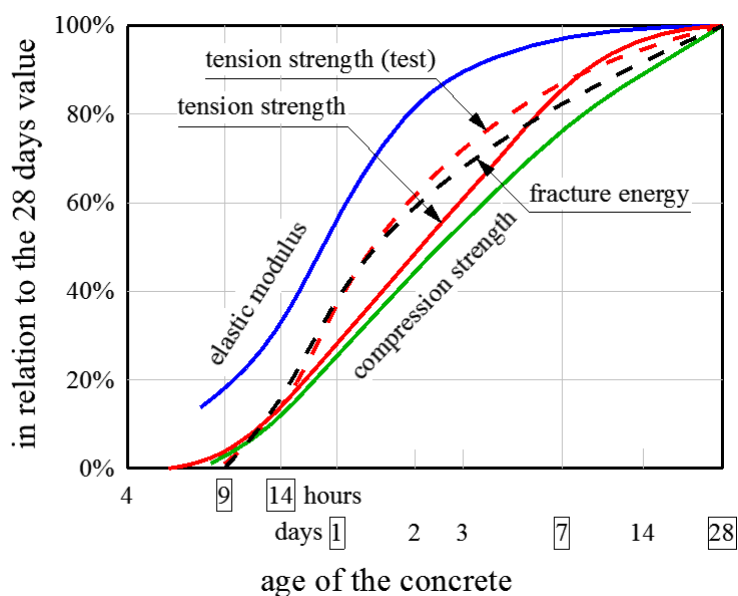


Fig. 2: The increase of the elastic modulus, compression strength, tension strength and fracture energy of the concrete as function of time in relation to the 28 days value [8, 5, 15]. Dashed lines are the results of the present research.

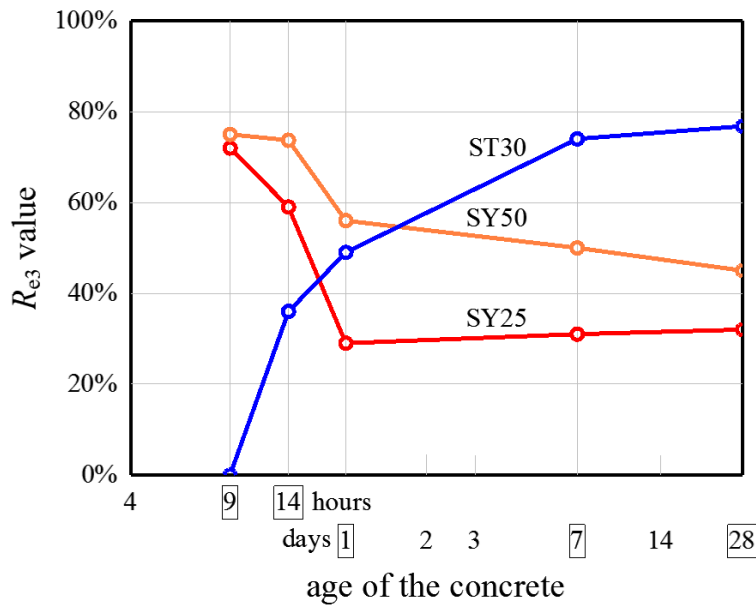


Fig. 3: The changes in the  $R_{e3}$  value of steel (ST) and synthetic (SY) reinforcement as a function of time

### 3. Finite element analysis

#### 3.1 Material model

The material model of concrete consists of a combined fracture-plastic failure surface [2]. Tension is handled herein by a fracture model, based on the classical orthotropic smeared crack formulation and the crack band approach. It employs the Rankine cube failure criterion with a fixed crack model (rotated crack model was not suitable for this calculation). The plasticity model of concrete in compression uses the William-Menétrey failure surface [11]. Aggregate interlock was taken into account by reducing the shear modulus with growing strain along the crack plane, according to the law formulated by Kolmar [10]. Although this does not cause notable changes in the results. The effect of the fibres was calculated with the modified fracture energy method [9]. The added fracture energy was calculated by inverse analysis.

All of these parameters of the plain and fibre reinforced concrete were implemented into a time-dependent material, where the parameters were changed in every step during the calculation. The parameters of the time-dependent material model could be seen in Table 4. Shrinkage strain was calculated according to Japanese standards [7] until day 232. Relative humidity was set to 60% and the water content was  $160 \text{ kg/m}^3$ .

Soil was modelled with a linear material model with an elastic modulus  $E=30\text{GPa}$ . Between the soil and the concrete there is a contact element (GAP) with three different types of strengths: 1) fix contact, *F-series*; 2) cohesion of 0.3 MPa, *M-series*; 3) cohesion of 0.06 MPa, *L-series*. The different contact elements are modelling the different subbases and layers under the concrete slab.

Tab.4: Time dependent material parameters

| Time  | Step  | Strain $\epsilon_{cs} \times 10^5$ | Elastic modulus $E$ [GPa] | Tension strength $f_t$ [MPa] | Compression strength $f_c$ [MPa] | Fracture energy $G_f$ [N/m] |
|-------|-------|------------------------------------|---------------------------|------------------------------|----------------------------------|-----------------------------|
| 9 h   | 20    | 1.91                               | 4.5                       | 0.0365                       | 1.14                             | 0.217                       |
| 14 h  | 258   | 2.59                               | 7.5                       | 0.38                         | 2.28                             | 12.1                        |
| 1 d   | 563   | 3.44                               | 16.5                      | 1.027                        | 9.5                              | 27.6                        |
| 7 d   | 2612  | 9.30                               | 29.1                      | 2.375                        | 28.5                             | 59.6                        |
| 28 d  | 5319  | 17.01                              | 30                        | 2.70                         | 38                               | 72.5                        |
| 232 d | 10020 | 30.39                              | 30                        | 2.70                         | 38                               | 72.5                        |

### 3.2 Numerical model and intervals

The industrial floor was modelled with ATENA Science FE software in 2D with plane strain idealisation. The dimensions and supports can be seen in Fig. 4. The mesh size was 6.66 cm (1/3 of the slab thickness) x 10 cm. Three main intervals were used: int-1) for calculating the own weight of the floor; int-2) for calculating until the end of the curing time; and int-3) for calculating until day 232.

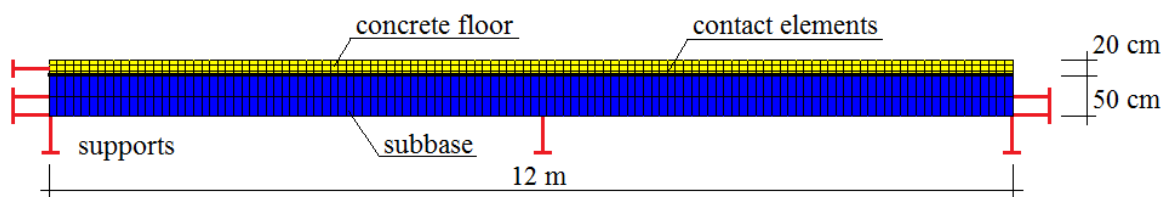


Fig. 4: Numerical model of the industrial floor

## 4. Results

The relationship between the dosage and the maximum crack at different contact element types can be seen in Fig. 5. The effect of fibre reinforcement shows significant differences at each type of contacts. The biggest effect can be reached at the soft connection, which is modelling the traditional industrial floor layers, e.g. 2 layers of PE folia. This effect goes up to even 30%, depending on the dosage. The dosage and maximum crack width shows direct proportionality. At the contact with medium stiffness the increase of dosage has limited advantages, thus low dosage seems to be the optimal solution. At fix contact there is no significant effect of the use of fibre. The crack propagation at plain concrete and FRC can be seen in Fig. 6. It is also notable that the displacement of the fibre reinforced concrete slab is bigger than the plain concrete at the free edge.

The increase of the crack width as a function of time could be seen in Fig. 7. This curve has the same characteristic as the time-shrinkage diagram. Obviously, there is no tearing at the connection in case of fix contact. The separation is a continuous process in case of soft connection, and results in a smooth curve, while, in case of medium connection the curve has a break point.

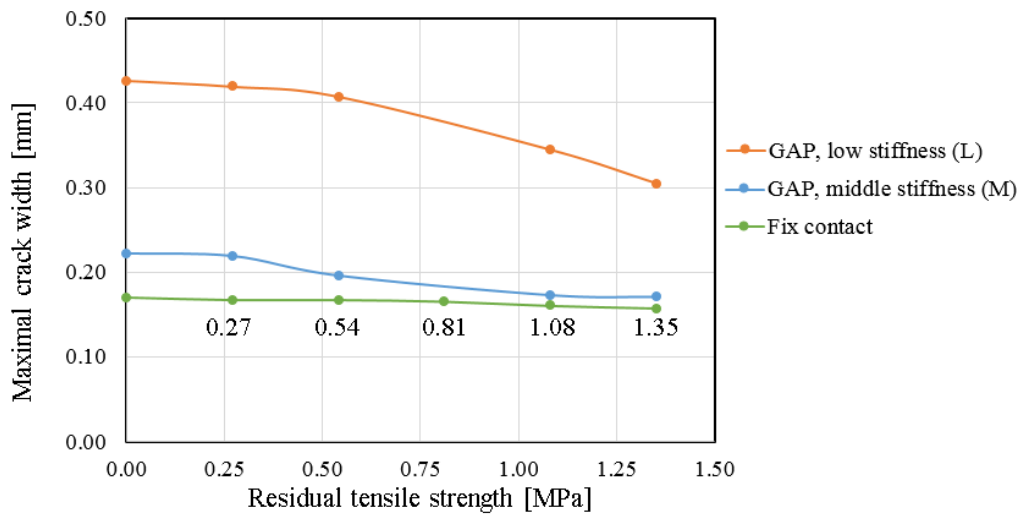


Fig. 5: Residual tensile strength and maximum crack width relationship

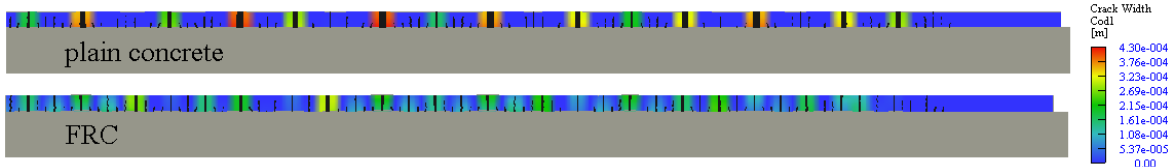


Fig. 6: Crack propagation at plain concrete and FRC

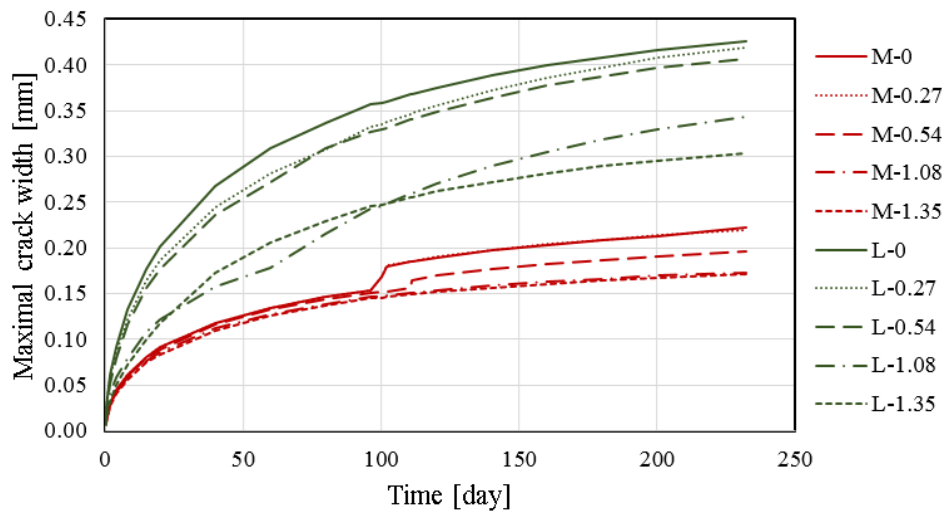


Fig. 7: Increase of crack width as a function of time

## 5. Conclusion

Effects of the fibres for preventing or reducing the early age cracking are well-know, although none of the standards or guidelines takes into account this advantage. After cracks appear the post-crack performance of the fibres are different: micro fibres have only limited residual tension strength, while macro fibres have significant value. The capacity of the fibres during hardening is also different, in this case it depends on the material: steel fibre has a limited capacity until the first day, while synthetic macro could work from the beginning of the life of the concrete. During the curing time of the concrete of an industrial

floor the concrete could crack. In this case micro fibres cannot prevent the crack opening, only macro fibres. The crack propagation and maximum crack width mostly depends on the fibre type, dosage and the connection between the floor and the subbase. The results of the beam tests were implemented into a time-dependent material model and FEA was done on a simple industrial floor structure. Results of the numerical research showed that also macro fibres have effect on the early age crack propagation, although these fibres mostly start working after the cracks appear. The maximum crack width and crack propagation were researched as a function of time. Research also showed that the effect of the fibre mostly depends on its dosage and the stiffness and strength of the contact between the industrial floor and subbase.

## References

- [1] ACI 209.2R-08, *Guide for Modeling and Calculating Shrinkage and Creep in Hardened Concrete*, ACI, 2008, pp. 18-22.
- [2] CERVENKA, J. and PAPANIKOLAOU V.K. Three dimensional combined fracture-plastic material model for concrete, in *International Journal of Plasticity* (24), 2008, pp. 2192-2220.
- [3] EN 1992 (Eurocode 2). Design of concrete structures, 2004, pp. 31-32.
- [4] International Federation for Structural Concrete (fib). *Model Code 2010 (Final Version)*, fib Bulletins 65 & 66, Lausanne, 2012, pp.145-148.
- [5] IVÁNYI Gy. (editor). *Erläuterungen zur DAfStb-Richtlinie Wasserundurchlässige Bauwerke aus Beton*, DAfStb, Heft 555, Beuth Verlag GmbH, Berlin-Köln, 2006.
- [6] Japan Society of Civil Engineers. *Method of test for flexural strength and flexural toughness of SFRC*, Standard JSCE SF-4, 1985.
- [7] Japan Society of Civil Engineers. *Standard specifications for concrete structures - 2007 "Design" JSCE Guideline for Concrete No.15*, 2010, pp. 50-55.
- [8] JÓZSA Zs. and FENYVESI O. Early age shrinkage cracking of fibre reinforced concrete, in *Concrete Structures* vol.11, 2010 pp. 61-66., ISSN: 1419-6441
- [9] JUHÁSZ K.P. Modified fracture energy method for fibre reinforced concrete, in: *Fibre Concrete 2013: Technology, Design, Application*. Prague 2013, pp. 89-90.
- [10] KOLMAR, W. *Beschreibung der Kraftuebertragung über Risse in nichtlinearen Finite-Element-Berechnungen von Stahlbetontragwerken*, Dissertation, T.H. Darmstadt, 1986.
- [11] MENÉTREY P. and WILLIAM K.J. Triaxial Failure Criterion for Concrete and Its Generalization, in *ACI Structural Journal*, 92(3), 1995, pp. 311-318.
- [12] Österreichische Vereinigung für Beton- und Bautechnik. *Richtlinie Faserbeton*, Österreichische Vereinigung für Beton- und Bautechnik, Wien 2008.
- [13] RAHMANI, T., BAKHSHI, M., MOBASHER, B. and SHEKARCHI M. Modeling early age drying in fiber reinforced concretes, in: *FRC 2014 Joint ACI-fib International Workshop, Fiber Reinforced Concrete: from Design to Structural Application*, 24-25 July 2014, Montreal, Canada, pp. 588-597.

- [14] SHAH, S.P, SARIGAPHUTI, M, and KARAGULER, M.E. Comparison of shrinkage cracking performance of different types of fibers and wiremesh, in *ACI SP-142*, 1994, pp. 1-18.
- [15] SPRINGENSCHMID, R. *Betontechnologie für die Praxis*, Berlin: Bauwerk, 2007.
- [16] SWAMY, R.N and STAVRIDES, H. Influence of fiber reinforcement on restrained shrinkage and cracking, in *ACI Journal*, 1979 March, pp. 443-460.
- [17] VANDEWALLE, L. et al. RILEM TC 162-TDF: Test and design methods for steel fibre reinforced concrete, in: *Materials and Structures*, Vol. 33., January-February, 3-5., 2002.
- [18] WEIGLER, H. and KARL, S. Junger Beton, Beanspruchung – Festigkeit Verformung, in *Betonwerk + Fertigteil-Technik*, 1974, No. 6. pp. 392-401 and No. 7. pp. 481-484.